R. & M. No. 3235

MINISTRY OF AVIATION

AERONAUTICAL RESEARCH COUNCIL
REPORTS AND MEMORANDA

On Axi-symmetrical Gas Jets, with Application to Rocket Jet Flow Fields at High Altitudes

By W. T. Lord

LONDON: HER MAJESTY'S STATIONERY OFFICE
1961
PRICE: 11s. 6d. NET

On Axi-symmetrical Gas Jets, with Application to Rocket Jet Flow Fields at High Altitudes

By W. T. Lord

Communicated by the Deputy Controller Aircraft (Research and Development), Ministry of Aviation

*Reports and Memoranda No. 3235**
July, 1959

Summary. A study is made of some existing analytical, numerical and experimental results for gas jets expanding out of axi-symmetrical nozzles. Jets expanding into a vacuum and into still air at finite pressure are considered in detail, and by introducing certain new ideas the existing results are expressed in a compact form and thereby rendered more widely applicable. A brief examination of jets expanding into supersonic airstreams suggests that some information about the flow fields of rocket jets at high altitudes may be deduced from the extended results for still-air jets in which the reference pressure at the nozzle exit is much greater than the ambient pressure; an example for a particular rocket and a specific trajectory is given.

1. *Introduction.* A study is made of the problem of a jet of perfect gas expanding out of an axi-symmetrical nozzle. The ratio of the specific heats of the jet gas is assumed to be constant. The nozzle may be divergent at the exit, and it is assumed to be surrounded by a coaxial circular cylinder with no annular space or base in the exit plane between the cylinder and the nozzle. The reference values of Mach number and pressure in the jet at the nozzle exit are taken to be the values at the surface of the nozzle immediately ahead of the exit.

The paper deals with jets expanding into a vacuum, into still air at finite pressure, and into air moving supersonically at a given Mach number and pressure. The discussion of jets expanding into a vacuum and into still air is fairly comprehensive, but the examination of jets expanding into supersonic airstreams is less detailed, being carried only as far as the establishment of a connection between rocket jets at high altitudes and still-air jets in which the reference pressure is much greater than the ambient pressure.

Concentration on expanding jets permits the assumption that the boundary layer inside the nozzle does not separate ahead of the geometrical exit of the nozzle. In the case of a jet expanding into still air, attention is focused on the initial portion of the jet from the nozzle exit to the neighbourhood of the cross-section at which the jet radius just attains a local maximum, and in this portion of the jet the influence of viscosity is small and may be neglected. Similarly, only the initial portion of a jet expanding into a supersonic stream is considered, and then in this case the effects of viscosity are confined to those produced by the boundary layer on the cylinder.

* Previously issued as R.A.E. Report No. Aero. 2626—A.R.C. 21,535, together with additional material from R.A.E. Tech. Memo. Aero. 625.

For theoretical purposes, the flow across the nozzle exit plane may be taken to be radial and it may be assumed that just at the nozzle lip there is a Prandtl-Meyer expansion. Then the flow in a jet can be calculated by the numerical method of characteristics, in conjunction with appropriate boundary conditions on the jet. Several specific jet-flow fields have been calculated by this method, mostly with the aid of an automatic computer; for example, jets expanding to vacuum have been calculated by Clippinger[1], and by Love and Grigsby[2]; jets expanding into still air by Love and Grigsby, Wang and Peterson[3], and Treutler[4]; jets expanding into supersonic airstreams by Wang and Peterson[3]. Other theoretical information on particular aspects of expanding jets has been given: for jets expanding into a vacuum by Owen and Thornhill[5], and Smith[6]; for jets expanding into still air by Love and others[2, 7, 8], and by Adamson and Nicholls[9]; for jets expanding into supersonic airstreams by Love[2, 10, 11].

In addition Love and Grigsby, and Adamson and Nicholls have given experimental information on jets expanding into still air, and Ladenburg, van Voorhis and Winckler[12] have determined experimentally the detailed flow fields of several jets expanding into still air; some experiments on jets expanding into supersonic airstreams have been reported by Love and Grigsby.

This paper presents an analysis of the theoretical and experimental information contained in these works*. It is found that by introducing certain new ideas it is possible to express the existing results in a compact form and thereby render them more widely applicable.

An illustration of the conditions near to the nozzle exit for an expanding jet is given in Fig. 1. The radial flow persists from the nozzle exit to the leading characteristic from the Prandtl-Meyer expansion at the nozzle lip.

A sketch of the flow field of a jet expanding to a vacuum is given in Fig. 2. The streamlines diverge and the Mach number increases along them. The contours of constant pressure, density and temperature are the same as the contours of constant Mach number.

Jets expanding into a vacuum are discussed in Section 2. The radial flow and the expansion at the nozzle lip can be calculated exactly and are well known, and only a few results relevant to the subsequent analysis are quoted here; these include, however, some new approximate results for the Prandtl-Meyer expansion which are useful for quick numerical calculations. The main property discussed is the distribution of Mach number along the axis downstream from the leading characteristic.

A sketch of the flow field of the initial portion of a jet expanding into still air is given in Fig. 3. At the nozzle lip the flow expands from the reference pressure to the ambient pressure. The boundary condition is that the pressure on the jet boundary is everywhere equal to the ambient pressure, and the necessity of achieving a boundary pressure much greater than that attained naturally in the expansion to a vacuum leads to the occurrence of shock waves within the jet. The shock-wave pattern shown in Fig. 3 is typical, although exceptions to it may occur when the reference pressure is not much greater than the ambient pressure; for instance, the shocks within the jet may be so near the nozzle exit that the leading characteristic does not reach the axis and, with nozzles of small divergence angle, the normal shock may not be present and the curved shock then extends to the axis. The shock waves may be regarded as dividing the jet into two regions. The outer region represents the total effect produced on the jet by the imposition of the finite ambient pressure. The inner region is unaffected by the ambient pressure and is a portion of the corresponding jet

* Ladenburg, van Voorhis and Winckler, and Love and Grigsby give extensive lists of references to other papers on jets which are not referred to specifically here.

which expands to a vacuum. Hence, flow fields of jets expanding into still air can be used to provide information about the flow near to the nozzle in jets expanding into a vacuum. As the reference pressure in the jet becomes very much greater than the ambient pressure the extent of the outer region dwindles and the inner region becomes the predominant portion of a still-air jet.

Jets expanding into still air are discussed in Section 3. The properties described are the shapes of the jet boundary and the shock waves. The shape of the jet boundary is taken to be determined by the initial direction angle at the nozzle lip and the location and value of the first maximum radius of the jet. The results for the initial direction angle follow directly from the conditions at the nozzle lip, and it is noted that the initial direction angle may be expressed very conveniently in terms of a particular parameter. Another parameter is found which enables formulae for the co-ordinates of the first jet maximum to be deduced from a vast number of jet boundaries calculated by the method of characteristics. A rough guide is given to the initial shape of the curved shock and the location and size of the normal shock.

For a jet expanding into a supersonic airstream there is, in the external stream, a shock wave which originates on the cylinder at or just upstream of the nozzle lip. The pressure on the jet boundary immediately downstream of the nozzle lip is therefore greater than the pressure in the undisturbed stream. The shock wave interacts with the boundary layer on the cylinder, and the form of the interaction depends on the values of the jet parameters and on the Mach number and pressure of the external flow. The jet boundary condition depends on the external shock-wave/boundary-layer system and on the relation between the shape of the jet boundary and the external flow downstream of the shock, and it is very difficult to express this condition satisfactorily. The external conditions lead, as in the case of a still-air jet, to the occurrence of shock waves within the jet. The shock-wave pattern inside the initial portion of the jet is of the same type as that inside a still-air jet, and in the inner region of the jet between the shock waves and the axis the flow is part of the corresponding jet expanding into a vacuum. The flow in the jet near the nozzle lip is controlled by the pressure on the jet boundary immediately downstream of the lip, and therefore the flow near the nozzle is the same as that in the corresponding jet expanding into still air at this particular pressure. Because of the different boundary conditions, the internal shock-wave patterns and the jet boundaries are not the same in the two jets, except near the nozzle lip. However, when the reference pressure is very much greater than the external pressure the inner region dominates a still-air jet, and it seems very likely that at high pressure ratios the flow in the portion of the corresponding still-air jet which is close to the nozzle exit is the same as the flow in that portion of the jet expanding into a supersonic stream.

There are some practical problems in which only a rough idea of the shape and structure of jets expanding into supersonic airstreams at high pressure ratios is required. For instance, in the estimation of radio-wave attenuation it is required to know the contours of constant density and temperature in rocket jets at high altitudes. This requirement may be satisfied by assuming that an idea of the variation of rocket jet flow fields with the rocket parameters and with altitude may be obtained by considering, instead of the actual jet with its appropriate values of external stream Mach number and pressure, the whole of the initial portion of the corresponding jet which expands into still air at the pressure on the actual jet boundary just downstream of the nozzle exit. The shock-wave/boundary-layer system in the external flow upstream of the nozzle exit then influences only the estimation of the relevant boundary pressure. Here, in Section 4, the correspondence between rocket jets and still-air jets is established by assuming that when the jet reference pressure is only

slightly greater than the boundary pressure there is an oblique shock attached to the nozzle lip, and that when the reference pressure is much greater than the boundary pressure there is a shock-wave/boundary-layer interaction on the cylinder upstream of the nozzle exit which gives the boundary pressure at the lip equivalent to that produced by a normal shock.

The information presented in this report may be used as the basis of a crude method of predicting rocket jet flow fields at high altitudes. A detailed account of such a method is not presented here but results for a practical example of a particular rocket and a specific trajectory are given.

2. *Jets Expanding into a Vacuum.* 2.1. *Region of Radial Flow.* The semi-divergence angle of the nozzle at the exit is denoted by θ_n, the ratio of the specific heats of the jet gas by γ_j, and the reference Mach number at the surface of the nozzle immediately ahead of the exit by M_j. The values of θ_n, γ_j and M_j may be chosen arbitrarily provided they are consistent with a possible nozzle flow, a condition which may be regarded as restricting the maximum value which θ_n may take for given values of γ_j and M_j; if $M_j = 1$ then for all γ_j the only permissible value of θ_n is zero, but for values of $M_j \geqslant 1{\cdot}5$ this restriction does not appear to be of practical importance. The radius of the nozzle at the exit is taken to be unity. The axial co-ordinate x is measured from the nozzle exit and the radial co-ordinate y is measured from the axis.

The basic solution of the radial flow stipulates that the streamlines are straight and appear to originate from the intersection of the axis and the tangent to the nozzle at the exit; the Mach number depends only on the radial distance from the apparent source. The information of primary interest in this investigation consists of the mass flow out of the nozzle, the shape of the leading characteristic from the nozzle lip, and the distribution of Mach number along the axis. Three auxiliary functions of the local Mach number M are involved: the area-ratio function λ defined by

$$\lambda = M\left[\frac{2}{(\gamma_j+1)} + \left(\frac{\gamma_j-1}{\gamma_j+1}\right)M^2\right]^{-(\gamma_j+1)/2(\gamma_j-1)}, \tag{1}$$

the Mach angle μ defined by

$$\mu = \sin^{-1}(M^{-1}), \tag{2}$$

and the Prandtl-Meyer angle ν defined by

$$\nu = \left(\frac{\gamma_j+1}{\gamma_j-1}\right)^{1/2}\tan^{-1}\left[\left(\frac{\gamma_j+1}{\gamma_j-1}\right)^{-1/2}(M^2-1)^{1/2}\right] + \cot^{-1}(M^2-1)^{1/2} - \frac{\pi}{2}; \tag{3}$$

λ and ν are adequately tabulated [13 to 18] for $1{\cdot}1 \leqslant \gamma_j \leqslant 5/3$.

The mass flow through the nozzle may be represented by the radius g of a uniform sonic stream with the same mass flow, and g is given by

$$g = [2(1-\cos\theta_n)]^{1/2}\operatorname{cosec}\theta_n\lambda_j^{1/2}. \tag{4}$$

If $\theta_n \leqslant 30$ deg, which it is likely to be in practice, this result may be approximated closely by

$$g = \lambda_j^{1/2}, \tag{5}$$

which shows that the mass-flow parameter g is effectively independent of θ_n.

The co-ordinates of a point on the leading characteristic can be expressed parametrically in terms of M, which varies from M_j at the lip to $\bar{M}$, say, on the axis, where $\bar{M}$ is defined by the relation

$$\bar{\nu} = \nu_j + 2\theta_n. \tag{6}$$

The parametric equations of the leading characteristic are

$$y = \lambda_j^{1/2} \sin(\theta_n + \tfrac{1}{2}\nu_j - \tfrac{1}{2}\nu)/\lambda^{1/2} \sin\theta_n, \tag{7}$$

$$\dot{x} = y \cot(\theta_n + \tfrac{1}{2}\nu_j - \tfrac{1}{2}\nu) - \cot\theta_n; \tag{8}$$

when $\theta_n = 0$ these equations reduce to the result $x = (1-y)\cot\mu$.

The distribution of Mach number along the axis is expressed by

$$x = (\lambda_j/\lambda)^{1/2} \operatorname{cosec}\theta_n - \cot\theta_n, \tag{9}$$

from $x = 0$ until $M = \bar{M}$ at $x = \bar{x}$ given by

$$\bar{x} = (\lambda_j/\bar{\lambda})^{1/2} \operatorname{cosec}\theta_n - \cot\theta_n; \tag{10}$$

when $\theta_n = 0$, $\bar{x} = \cot\mu_j$ and $M = M_j$ for $0 \leqslant x \leqslant \cot\mu_j$.

2.2. *Conditions at the Nozzle Lip.* In terms of M, for $M_j \leqslant M \leqslant \infty$, the flow direction θ at the nozzle lip is given by

$$\theta = \theta_n + \nu - \nu_j, \tag{11}$$

and the characteristic direction ϕ is given by

$$\phi = \theta - \mu. \tag{12}$$

In the vacuum, $M = \infty$, $\mu = 0$ and $\nu = \nu_{\max}$ where

$$\nu_{\max} = \left[\left(\frac{\gamma_j + 1}{\gamma_j - 1}\right)^{1/2} - 1\right]\frac{\pi}{2}. \tag{13}$$

The obvious way of calculating the conditions at the lip is to specify M and to find ν from tables[13 to 18]. However, in addition to the local Mach number at a point, the local values of pressure p, density ρ and temperature T are also important, and there is a simpler way of calculating the ratios of these quantities to their reference values p_j, ρ_j and T_j than by specifying M. Let τ denote the ratio of the local speed of sound to the stagnation sound speed in the jet, and let τ_j be its value on the nozzle immediately ahead of the exit. Also, let the quantities s and N_j be defined by

$$s = \tau/\tau_j, \tag{14}$$

$$\gamma_j = (N_j + 2)/N_j. \tag{15}$$

Then it follows that

$$p/p_j = s^{N_j+2}, \quad \rho/\rho_j = s^{N_j}, \quad T/T_j = s^2. \tag{16}$$

It may be deduced from these relations that in the numerical calculation of these ratios it is advantageous to choose γ_j so that N_j is an integer and to consider s as the primary-state parameter. When s is specified the corresponding value of M is obtained by first calculating τ_j from the relation

$$\tau_j = [1 + \tfrac{1}{2}(\gamma_j - 1)M_j^2]^{-1/2}, \tag{17}$$

then forming $\tau = s\tau_j$, and finally using the equation

$$M = [2(\gamma_j - 1)^{-1}(\tau^{-2} - 1)]^{1/2}. \tag{18}$$

Figs. 4 and 5 are included to facilitate the calculation of M in this manner.

When numerous values of s are specified it may often be quicker than calculating M and extracting ν from tables, and sufficiently accurate, to evaluate ν directly from s by the following approximate method. Consider $(\nu-\nu_j)/(\nu_{\max}-\nu_j) = \sigma$, say, as a function of s for $1 \geqslant s \geqslant 0$. For s near 1 and 0 respectively

$$\sigma = S_1(1-s) + \ldots., \quad \text{where } S_1 = 2(\gamma_j-1)^{-1} M_j^{-2}(M_j^2-1)^{1/2} (\nu_{\max}-\nu_j)^{-1}, \tag{19}$$

$$\sigma = 1 - S_0 s + \ldots., \quad \text{where } S_0 = 2(\gamma_j-1)^{-1} [2(\gamma_j-1)^{-1} + M_j^2]^{-1/2} (\nu_{\max}-\nu_j)^{-1}. \tag{20}$$

Inspection of the numerical values of S_1 and S_0 displayed in Figs. 6 and 7 shows that $S_1 \geqslant 1$ except for M_j less than about $[1+9(\gamma_j-1)/20]$ while $S_0 \leqslant 1$ for all M_j, and in many cases when $S_1 \geqslant 1$ it is satisfactory to find σ by drawing a faired curve between the behaviours near $s = 1$ and $s = 0$. An example of the usefulness of this procedure, in an unfavourable case, is given in Fig. 8. The accuracy here is extraordinarily good, but there may have been some luck involved in the fairing. The possibility of bad luck can be effectively eliminated by calculating σ exactly at an intermediate point, say $s = \sqrt{\frac{1}{2}}$ because the region near $s = 1$ is the more difficult to predict. If such a point is calculated exactly, the method of approximation by drawing a faired curve may apply when $S_1 < 1$.

It can be shown that $\sigma \to (1-s)$ as $M_j \to \infty$ for all $\gamma_j \neq 1$ and all s, and indeed it happens that the simple relation

$$\sigma = \frac{\nu - \nu_j}{\nu_{\max} - \nu_j} = 1 - s \tag{21}$$

gives a quick rough guide to the size of ν provided that M_j and s are not both too near to 1. The quantity $(\nu_{\max}-\nu_j)$ is shown in Fig. 9.

2.3. *Mach Number Distribution along the Axis.* 2.3.1. *Distribution near to the radial flow.* The variation of $(M-\bar{M})$ with $(x-\bar{x})$ along the axis just downstream of the end of the radial flow in the flow fields of Clippinger[1], Wang and Peterson[3], and Treutler[4], which involve values of θ_n, γ_j and M_j in the ranges $0 \leqslant \theta_n \leqslant 15$, $1{\cdot}15 \leqslant \gamma_j \leqslant 1{\cdot}4$ and $1 \leqslant M_j \leqslant 5$, can be expressed roughly by the following formulae:

$$(M-\bar{M}) = J(\theta_n, \gamma_j, M_j)(x-\bar{x}) + \ldots., \tag{22}$$

$$J = G(\gamma_j, M_j) f_1(M_j) f_2(\theta_n, \gamma_j, M_j), \tag{23}$$

$$G = 2(\gamma_j+1)^{-1} (1-M_j^{-2})^{1/2} [\tfrac{1}{2}(\gamma_j-1) + M_j^{-2}], \tag{24}$$

$$f_1 = \frac{4}{9}(19-15M_j^{-1}), \tag{25}$$

$$f_2 = 2\,[1 + (1+\bar{x}^2)M_j^{-2}]^{-1}. \tag{26}$$

The function G is obtained from the corresponding Mach number distribution in the two-dimensional Prandtl-Meyer expansion of a uniform stream of Mach number M_j round a single corner, and is shown in Fig. 10. The function f_1 is an empirical factor giving the modification due to axial symmetry when $\theta_n = 0$. The function f_2 is a further empirical factor which represents the effect of θ_n in the axi-symmetrical case; $\bar{x}$ is given in terms of θ_n, γ_j and M_j by Equation (10).

The result for $\theta_n \neq 0$ is very rough indeed, being based on only three cases, all with $\theta_n = 15$ deg. For $\theta_n = 0$, the formulae have a rather firmer foundation. In this case $f_2 = 1$, and the values of

J/G for five of Wang and Peterson's examples are compared with f_1 in Fig. 11. The value $f_1 = 16/9$ when $M_j = 1$ is obtained by assuming that the following formula

$$x = 2\nu^{-1}(\lambda^{-1/2} - 1), \tag{27}$$

which may be shown to fit approximately the numerical results of Clippinger[1] for $1 \leqslant M \leqslant 10$ in the case $\gamma_j = 1{\cdot}4$, holds for all γ_j.

2.3.2. *Distribution far from the radial flow.* It may be argued that at large distances from the radial flow the way in which the Mach number varies depends only on the mass flow through the nozzle and on the properties of the jet gas; that is, for a given mass-flow parameter g the variation of $(M - \bar{M})$ for large $(x - \bar{x})$ may be independent of θ_n and M_j and depend only on γ_j. On the basis of this argument it follows that the variation of $(M - \bar{M})$ for large $(x - \bar{x})$ is given by the case in which $\theta_n = 0$ and $M_j = 1$. But it may be shown that when $\gamma_j = 1{\cdot}4$ the axial Mach number distribution at large distances from a sonic nozzle becomes the distribution of the equivalent radial flow which has the same mass-flow parameter g for its flow between the axis and the streamline inclined to the axis at the angle $\frac{1}{4}\nu_{\max}$. It seems reasonable to assume that this result holds for all γ_j. The axial Mach number distribution of such an equivalent radial flow is expressed exactly by

$$(x - \bar{x}) = [2(1 - \cos\tfrac{1}{4}\nu_{\max})]^{-1/2}(\lambda^{-1/2} - \bar{\lambda}^{-1/2})g, \tag{28}$$

which may be approximated closely, using Equation (5), by

$$(x - \bar{x}) = [2(1 - \cos\tfrac{1}{4}\nu_{\max})]^{-1/2}\lambda_j^{1/2}(\lambda^{-1/2} - \bar{\lambda}^{-1/2}). \tag{29}$$

From this it may be shown that for large $(x - \bar{x})$ the axial Mach number distribution of an axisymmetrical jet expanding to a vacuum is given by the expression

$$(M - \bar{M}) = K(x - \bar{x})^{(\gamma_j - 1)} + \ldots, \tag{30}$$

where

$$K = \{\lambda_j^{-1}[2(1 - \cos\tfrac{1}{4}\nu_{\max})]\}^{(\gamma_j - 1)/2}[(\gamma_j + 1)/(\gamma_j - 1)]^{(\gamma_j + 1)/4}. \tag{31}$$

The numerical results of Wang and Peterson appear to confirm this result.

2.3.3. *Distribution along the entire axis.* Adamson and Nicholls[9] suggest that for a jet expanding out of a conical nozzle the Mach number distribution along the entire axis, beyond the radial flow, is the same as the Mach number distribution for a jet with the same mass-flow parameter expanding out of a sonic nozzle. At large distances this gives the same behaviour as that suggested here. However, it leads to the result that the Mach number distribution downstream of the radial flow is effectively independent of θ_n for all $(x - \bar{x})$, whereas Equations (22) to (26) indicate that θ_n has a large effect at least for small $(x - \bar{x})$.

An alternative suggestion which gives an idea of the Mach number distribution along the entire axis is to transform to other variables which have finite ranges and which have a linear relationship at the ends of the ranges. An example of such a transformation is given by the substitutions

$$\xi = 1 - [1 + (x - \bar{x})]^{-(\gamma_j - 1)}, \tag{32}$$

$$\eta = [1 + (M - \bar{M})^{-1}]^{-1}. \tag{33}$$

Then $\xi = 0, 1$ when $(x-\bar{x}) = 0, \infty$ and $\eta = 0, 1$ when $(M-\bar{M}) = 0, \infty$; the behaviours of η for ξ near 0 and 1 are

$$\eta = (\gamma_j - 1)^{-1} J\xi + \ldots, \tag{34}$$

$$\eta = 1 - K^{-1}(1-\xi) + \ldots . \tag{35}$$

The first steps in drawing an entire Mach number distribution are then to plot the behaviours of η near $\xi = 0, 1$ in the $\xi - \eta$ plane. It may then be possible in some cases to draw a faired curve between the two extremes with reasonable confidence without further information. However, the curve in the $\xi - \eta$ plane may have an inflection and so such a procedure is not always satisfactory. Therefore it is worthwhile to obtain an intermediate point, and the value $\xi_{1/2}$ for which $\eta = \frac{1}{2}$ is recommended. However, there is not enough information available to enable a formula for $\xi_{1/2}$ to be concocted for useful ranges of θ_n, γ_j and M_j, but Fig. 12 contains some values from Wang and Peterson's examples and from Equation (27), and these may be of some use for general guidance.

3. *Jets Expanding into Still Air at Finite Pressure.* When the air outside the jet is at a non-zero pressure, the jet depends on θ_n, γ_j and M_j and on the parameter p_j/p_b, where p_j is the jet reference pressure and p_b is the ambient pressure. For expanding jets $p_j/p_b \geqslant 1$.

3.1. *Jet Boundary.* The determining properties of a jet boundary appear to be the initial direction angle θ_b and the location $x_{\max}$ and value $y_{\max}$ of the first maximum radius of the jet. Here, formulae are given which allow θ_b and $x_{\max}$ and $y_{\max}$ to be calculated for wide ranges of the parameters.

3.1.1. *Initial direction angle.* The initial direction angle can be deduced directly from the conditions at the nozzle lip in the jet expanding to a vacuum. The initial direction angle θ_b is the value of θ which corresponds to the pressure p_b on the boundary, so that θ_b may be written

$$\theta_b = \theta_n + \theta_{b\,0}, \tag{36}$$

where $\theta_{b\,0}$ is the value of θ_b when $\theta_n = 0$ and is given by

$$\theta_{b\,0} = \nu_b - \nu_j; \tag{37}$$

the maximum possible value of $\theta_{b\,0}$, attained in the expansion to a vacuum, is

$$\theta_{b\,0\,\max} = \nu_{\max} - \nu_j; \tag{38}$$

The numerical values of $\theta_{b\,0\,\max}$ are shown in Fig. 9. If s_b is defined by

$$s_b = (p_b/p_j)^{(\gamma_j - 1)/2\gamma_j}, \tag{39}$$

and s_b is specified rather than p_j/p_b itself, then θ_b can be calculated from s_b in the same way as θ is calculated for a given value of s, the calculation of M_b being an intermediate step. Similarly the approximate methods of Section 2.2 apply, and it follows that the expression

$$\theta_b = \theta_n + \theta_{b\,0\,\max}(1 - s_b) \tag{40}$$

gives an estimate of θ_b for all θ_n, γ_j, M_j and s_b except when both M_j and s_b are too near to unity.

3.1.2. *Location and size of the first maximum of the jet radius.* Love, Woodling and Lee[7] present the results of calculations by the method of characteristics of 2,960 jet boundaries, covering the

following values of the parameters: $\theta_n = 5$ deg, 10 deg, 15 deg, 20 deg; $\gamma_j = 1{\cdot}115$, $1{\cdot}2$, $1{\cdot}3$, $1{\cdot}4$, $5/3$; $M_j = 1{\cdot}5$, 2, $2{\cdot}5$, 3; $p_j/p_b = 1(0{\cdot}25)10$. An examination of these boundaries has led to formulae being established for $x_{\max}$ and $y_{\max}$ for these ranges of θ_n, γ_j, M_j and p_j/p_b.

The dominant parameter is p_j/p_b. From a result of Love and Grigsby[2] and from the calculations of Love, Woodling and Lee it appears that both $x_{\max}$ and $y_{\max}$ tend to infinity like $(p_j/p_b)^{1/2}$ as $p_j/p_b \to \infty$, for all θ_n, γ_j and M_j. This behaviour is also consistent with the behaviour of the normal shock location discussed later. Therefore a convenient way to express the results for $x_{\max}$ and $y_{\max}$ is to consider the quantities

$$X = x_{\max 1}/x_{\max}, \tag{41}$$

$$Y = y_{\max 1}/y_{\max}, \tag{42}$$

where the subscript 1 denotes the value when $p_j/p_b = 1$, as functions of the parameter t_b defined by

$$t_b = (p_b/p_j)^{1/2}. \tag{43}$$

Then both X and Y are zero when $t_b = 0$ and unity when $t_b = 1$.

The results of Love, Woodling and Lee for $x_{\max 1}$ and $y_{\max 1}$ can be represented approximately by the formulae

$$x_{\max 1} = \frac{7}{10} M_j, \tag{44}$$

$$y_{\max 1} = 1 + \frac{7}{20} M_j \tan \theta_n. \tag{45}$$

Since the values of X and Y are known at $t_b = 0$ and $t_b = 1$, it is assumed that their behaviours for intermediate values of t_b can be typified by their values at $t_b = \frac{1}{3}, \frac{1}{2}$ and their derivatives at $t_b = 1$. These quantities can be obtained from the calculations of Love, Woodling and Lee for $p_j/p_b = 9$, 4 and for p_j/p_b near 1. Letting a subscript denote the value of a quantity at that value of t_b, and with a dash denoting differentiation with respect to t_b, it is found that the following formulae display the main features of the data;

$$X_{1/3} = \frac{1}{3840}(6+M_j)[(70+9\gamma_j) + 14(9\gamma_j - 10)\tan\theta_n] \tag{46}$$

$$X_{1/2} = \frac{1}{20}[5 + 2(2\gamma_j + M_j - 3)\tan\theta_n] \tag{47}$$

$$X_1' = \frac{1}{9}(10 - 27\tan\theta_n + 45\tan^2\theta_n)\gamma_j^{-1/2}[(5M_j - 3)M_j^{-2}(M_j^2-1)^{1/2}]\left\{\frac{7}{10}M_j\right\}^{-1} \tag{48}$$

$$Y_{1/3} = \frac{1}{300}[15(4\gamma_j+1) - 2(2M_j-3)(5-3\gamma_j)(1-5\tan\theta_n)] \tag{49}$$

$$Y_{1/2} = \frac{1}{21600}(7\gamma_j - M_j + 10)(20 + 7M_j\tan\theta_n)[30 - 10\tan\theta_n - 3(7\gamma_j + 3M_j - 12)\tan^2\theta_n] \tag{50}$$

$$Y_1' = \frac{28}{25}(1+\tan\theta_n)\gamma_j^{-1}[M_j^{-1}(M_j^2-1)^{1/2}]\left\{1 + \frac{7}{20}M_j\tan\theta_n\right\}^{-1}. \tag{51}$$

The above forms for $X_{1/3}$, $X_{1/2}$, $Y_{1/3}$, $Y_{1/2}$ have been derived crudely, any simple satisfactory variation with each parameter being accepted and in several instances this turned out to be linear. Rather more care has been taken with the derivations of $x_{\max 1}$, $y_{\max 1}$, X_1', Y_1' since they have been arranged to exhibit two well-established features for p_j/p_b near 1, namely that the shapes of jet

boundaries with the same initial direction angle are practically independent of γ_j and that jet boundaries can be represented by circular arcs with the correct values of θ_b, $x_{\max}$ and $y_{\max}$. However, there has been no attempt to express the separate formulae (46) to (51) in such a way that consistent trends with respect to θ_n, γ_j and M_j may be discerned, and probably more consistent formulae may be obtained by inspecting the given formulae and making slight adjustments within the tolerances allowed by their inaccuracy.

For the variation of X and Y with p_j/p_b within the range $1 \leqslant p_j/p_b \leqslant 9$ some form of interpolation with respect to t_b may be used. In Fig. 13 an indication is given of the accuracy of interpolating X and Y by a quartic in t_b, for the particular example $p_j/p_b = 5$ selected by Love, Woodling and Lee.

Care must be taken in attempting to use the formulae for values of the parameters outside the stated ranges. The range of γ_j is probably adequate, for practical purposes. Extrapolation with respect to M_j is not recommended, but extrapolation down to $\theta_n = 0$ is probably reasonable. Some idea of the behaviours of $x_{\max}$ and $y_{\max}$ for values of $p_j/p_b > 9$ should be possible, and it is suggested that for rough analytical purposes the order of $x_{\max}$ and $y_{\max}$ for $p_j/p_b > 9$ may be obtained by taking

$$X = 3X_{1/3}t_b, \tag{52}$$

$$Y = 3Y_{1/3}t_b. \tag{53}$$

3.2. *Shock Waves in the Jet.* 3.2.1. *Initial shape of the curved shock.* The initial inclination of the curved shock is the inclination ϕ_b of the final characteristic at the nozzle lip, which may be found easily when θ_b is known from the relation

$$\phi_b = \theta_b - \mu_b. \tag{54}$$

An examination of the positions of the curved shock in various cases[2, 8], not discussed here, indicates that an idea of the initial shape of the curved shock can be obtained from the initial inclination and the shape of the corresponding jet boundary.

3.2.2. *Location and size of the normal shock.* Adamson and Nicholls[9] suggest that the normal shock occurs in such a position that the pressure behind it is equal to the ambient pressure p_b. This suggestion appears to be a very useful guide. It means that if the axial Mach number distribution of the jet expanding to a vacuum can be estimated, in a manner such as that outlined earlier for instance, then the distance l of the normal shock from the exit plane of the nozzle can be found immediately.

The analytical expression given by (30) and (31) for the form of the axial Mach number distribution at large distances from the radial flow enables an analytical expression for l for large values of p_j/p_b to be derived. If M_s and p_s are the Mach number and pressure on the axis immediately in front of the normal shock then if the pressure behind the shock is p_b it follows that

$$p_b/p_s = 2\gamma_j(\gamma_j+1)^{-1}M_s^2 - (\gamma_j-1)/(\gamma_j+1), \tag{55}$$

and since p_s is related to p_j by

$$p_s/p_j = [1 + \tfrac{1}{2}(\gamma_j-1)M_j^2]^{\gamma_j/(\gamma_j-1)}\,[1 + \tfrac{1}{2}(\gamma_j-1)M_s^2]^{-\gamma_j/(\gamma_j-1)} \tag{56}$$

then p_b/p_j and M_s are related by

$$p_b/p_j = [2\gamma_j(\gamma_j+1)^{-1}M_s^2 - (\gamma_j-1)/(\gamma_j+1)]\,[1 + \tfrac{1}{2}(\gamma_j-1)M_j^2]^{\gamma_j/(\gamma_j-1)} \times \\ \times\,[1 + \tfrac{1}{2}(\gamma_j-1)M_s^2]^{-\gamma_j/(\gamma_j-1)} \tag{57}$$

For large values of M_s this becomes

$$p_b/p_j = 2\gamma_j(\gamma_j+1)^{-1}[2(\gamma_j-1)^{-1} + M_j^2]^{\gamma_j/(\gamma_j-1)} M_s^{-2/(\gamma_j-1)} + \ldots . \quad (58)$$

The axial Mach number distribution gives

$$M_s = Kl^{(\gamma_j-1)} + \ldots , \quad (59)$$

and hence combining these two results it follows that for large p_j/p_b

$$l = L(p_j/p_b)^{1/2} + \ldots , \quad (60)$$

where

$$L = K^{-1/(\gamma_j-1)}[2\gamma_j(\gamma_j+1)^{-1}]^{1/2}[2(\gamma_j-1)^{-1} + M_j^2]^{\gamma_j/2(\gamma_j-1)} . \quad (61)$$

Since it might be expected that l would vary in the same way as $x_{\max}$ for large values of p_j/p_b, this result helps to confirm the assumed variation of $x_{\max}$ with $(p_j/p_b)^{1/2}$ when p_j/p_b is large.

Love and Grigsby[2] give a large amount of experimental information on the location of the normal shock in the particular case when $\gamma_j = 1{\cdot}4$ for $\theta_n = 0(5 \text{ deg})20 \text{ deg}$, $M_j = 1{\cdot}0(0{\cdot}5)3{\cdot}0$ and for various values of p_j/p_b in the range $1 \leqslant p_j/p_b \leqslant 100$. The results indicate that θ_n has only a very small effect on l. The measured values of l in the case $\theta_n = 0$ are illustrated in Fig. 14 in the form of $l/x_{\max}$ as a function of t_b, the values of $x_{\max}$ being calculated from Equations (41), (44), (46), (47), (48). Also included is the rough result obtained for $t_b = 0$ by using Equations (60), (61), (41), (44) and (52); it is effectively independent of M_j in the range considered.

In the case of the size of the normal shock, defined by its radius d, the results of Love and Grigsby[2] for $\gamma_j = 1{\cdot}4$ show complicated variations with p_j/p_b and M_j and also with θ_n when $p_j/p_b < 4$, and in this range of p_j/p_b information is best obtained directly from the original paper. The results for $p_j/p_b \geqslant 4$ can be condensed and extended somewhat, but no reliable and simple formulae have been deduced. However, it appears that d becomes infinite like $(p_j/p_b)^{1/2}$ as $p_j/p_b \to \infty$ and at least for large values of p_j/p_b it is useful to consider the quantity $d/y_{\max}$.

4. *Jets Expanding into Supersonic Airstreams.* 4.1. *Application to Rocket Jets at High Altitudes.* Consider a missile which has a single axi-symmetrical rocket motor, with its external surface cylindrical ahead of the nozzle exit and with no annular space or base in the exit plane. Assume that the cylindrical portion of the missile is long enough for the flow conditions on the external surface upstream of the nozzle exit to be the same as those relative to the missile in the surrounding air, and let M_∞ and p_∞ denote the Mach number and pressure in the external flow. The aerodynamics of the rocket jet then depend on θ_n, γ_j, M_j, p_j/p_∞ and M_∞.

For a missile moving in a given trajectory, the quantities θ_n, γ_j, M_j and p_j depend on the particular rocket and are independent of the altitude, while p_∞ depends on the altitude but is independent of the trajectory, and M_∞ depends on the altitude through the trajectory. If the pressure of the atmosphere at sea level is denoted by $p_{\infty 0}$, then p_j/p_∞ may be written as $p_j/p_{\infty 0}$ multiplied by $p_{\infty 0}/p_\infty$, which depends only on the altitude. Therefore, the practical independent parameters are θ_n, γ_j, M_j, $p_j/p_{\infty 0}$ and the altitude.

Now in the estimation of radio-wave attenuation, for instance, there is a requirement for a rapid method of predicting the contours of constant density and temperature in rocket jets at high altitudes. But the flow near the nozzle in a jet expanding into a supersonic stream is the same as that in the corresponding jet expanding into still air at the pressure p_b on the actual jet boundary just downstream of the nozzle lip, and the region in which the two jets are identical gets bigger as

the pressure ratio increases. Moreover, the information given here is sufficient to enable an idea of the boundaries and shock waves of still-air jets to be obtained and also, using the information on vacuum jets, the contours of constant density and temperature in the inner region to be estimated. Therefore, it is possible to get an idea of rocket jet flow fields at high altitudes by relating p_b to the altitude. A composite picture (subject of course to the limitation of continuum flow theory) may be formed which has the flow field of the corresponding vacuum jet as a background and has superimposed on it the jet boundaries and shock waves for the still-air jets with values of p_j/p_b corresponding to certain values of altitude. The condition that the jet suffers no deflection just at the nozzle lip defines the lowest altitude which may be considered.

A method of calculating a variation of p_j/p_b with altitude is now given. It is assumed, as by Love[10], than when $p_j/p_b = 1$, which occurs between about 40,000 to 50,000 feet, there is in the external stream an oblique shock attached to the nozzle lip, and it is further assumed that the oblique shock does not immediately become detached at p_j/p_b increases above 1. These assumptions imply the existence of a maximum permissible value of $p_j/p_{\infty 0}$ for a given θ_n, but the restriction does not turn out to be serious. At altitudes above about 100,000 feet the attached oblique shock configuration would not be maintained and there would be a shock and separated boundary-layer system on the cylinder ahead of the nozzle exit. The maximum flow-deflection angle through an oblique shock may be used to give a rough criterion for the breakdown of the attached shock assumption. In order to get an idea of the boundary pressure in these circumstances at altitudes well away from the lowest it is assumed, following Love and Lee[8], that the pressure rise is equivalent to that through a normal shock. No hypothesis is made about the precise external flow pattern at intermediate altitudes.

It appears from the United States' extension to the I.C.A.O. standard atmosphere[19] that, if h denotes the altitude in millions of feet, a close approximation to the ambient static pressure p_∞ is given for $0 \leqslant h \leqslant 0{\cdot}4$ by

$$p_\infty/p_{\infty 0} = 10^{-19h} = \mathrm{e}^{-h/0{\cdot}0228}. \tag{62}$$

Therefore, up to 400,000 feet, the altitude is given in terms of p_j/p_∞ and $p_j/p_{\infty 0}$ by

$$h = 0{\cdot}0228[\log_e p_j/p_\infty - \log_e p_j/p_{\infty 0}]. \tag{63}$$

Hence the problem of finding a relationship between p_j/p_b and h becomes that of relating p_j/p_b and p_j/p_∞.

In order to obtain explicit results a specific trajectory is now assumed; a similar analysis to that which follows could easily be carried out for any other trajectory (or indeed for a wind-tunnel experiment in which M_∞ is constant). It appears that the simple relation

$$M_\infty = h/0{\cdot}0228, \qquad 0 \leqslant h \leqslant 0{\cdot}4 \tag{64}$$

defines a realistic trajectory, and in this case it follows that M_∞ and p_j/p_∞ are connected by

$$M_\infty = \log_e p_{\infty 0}/p_j - \log_e p_\infty/p_j. \tag{65}$$

Consider first the range near $p_b/p_j = 1$. Suppose that the pressure change through an oblique shock is written $p_b/p_\infty = P(M_\infty, \theta_b)$; the function P is known numerically[13,14] and approximately analytically[15]. When $p_b/p_j = 1$, $\theta_b = \theta_n$ since the jet is not in this circumstance deflected initially. Therefore, if $M_{\infty 1}$ denotes the value of M_∞ when $p_b/p_j = 1$ and if P_1 denotes $P(M_{\infty 1}, \theta_n)$, then for the particular trajectory under consideration it follows that $M_{\infty 1}$ is defined as a function of $p_{\infty 0}/p_j$ and θ_n by the implicit equation

$$M_{\infty 1} = \log_e p_{\infty 0}/p_j + \log_e P_1. \tag{66}$$

To ensure that a well-established attached oblique shock is present when $p_b/p_j = 1$ it is stipulated, for convenience, that $p_{\infty 0}/p_j$ must be such that $M_{\infty 1}$ is greater than the value, $(M_{\infty 1})_{\min}$ say, at which $\partial P_1/\partial M_{\infty 1} = 0$. This means that, if $(P_1)_{\min}$ denotes $P\{(M_{\infty 1})_{\min}, \theta_n\}$, then

$$p_j/p_{\infty 0} \leqslant (P_1)_{\min} \exp\{-(M_{\infty 1})_{\min}\}. \tag{67}$$

It may be shown, by matching the oblique shock relations with the Prandtl-Meyer expansion of the jet at the nozzle lip, and using the relation between M_∞ and p_∞/p_j, that for values of p_b/p_j near 1

$$p_\infty/p_j = P_1^{-1}[1 - \{P_1 + \gamma_j^{-1} M_j^{-2}(M_j^2 - 1)^{1/2}\dot{P}_1\}(P_1 - P_1')^{-1}(1 - p_b/p_j) + \ldots .], \tag{68}$$

where $P_1' = \partial P_1/\partial M_{\infty 1}$ and $\dot{P}_1 = \partial P_1/\partial \theta_n$ and both P_1' and $\dot{P}_1$ can be obtained from the existing information [13, 14, 15] on P_1.

When p_b/p_j is very small it is assumed that there is a shock-wave/boundary-layer interaction on the cylinder upstream of the nozzle exit such that the pressure at the nozzle exit is that appropriate to the pressure rise through a normal shock; then it follows, by using Equation (65), that

$$p_b/p_j = \tfrac{7}{6}(p_\infty/p_j)\log_e^2 p_\infty/p_j + \ldots . \tag{69}$$

Having related p_b/p_j and p_∞/p_j, the final requirement is to relate p_b/p_j and h. The above results yield relations for p_b/p_j for values of h near its minimum value $h_1 = 0{\cdot}0228 M_{\infty 1}$ and for higher values of h corresponding to p_b/p_j small. For intermediate values of h these end results can easily be connected by graphical interpolation.

4.2. *Example.* The information given in this paper may be used as the basis of a crude method of predicting rocket jet flow fields at high altitudes. Such a method has been evolved but the details, which are of an essentially expedient nature, have not been published (although they are available as an unpublished Memorandum). Here the results of a practical example for a particular rocket and a specific trajectory are reproduced.

The example considered is the case for which the semi-divergence angle of the nozzle θ_n is 15 deg, the ratio of specific heats of the jet gas γ_j is 1·2, the jet reference Mach number M_j is 3, the jet reference pressure p_j is one third of atmospheric pressure at sea level $p_{\infty 0}$, and the trajectory is that assumed above in which the external Mach number M_∞ varies linearly with altitude up to a value of about 18 at 400,000 feet. The jet begins to expand out of the nozzle at about 43,000 feet, and the calculations apply between this altitude and 400,000 feet. The variation of p_j/p_b with altitude is shown in Fig. 15, and the variations of θ_b, ϕ_b, $x_{\max}$, $y_{\max}$, l and d are shown in Fig. 16; the jet boundaries and internal shock-wave patterns for some altitudes from 100,000 feet to 400,000 feet are drawn on the basic map of constant density and temperature contours in Fig. 17. The initial direction angle of the jet varies almost linearly with altitude, from 15 deg at 43,000 feet to 105 deg at 400,000 feet. The maximum radius of the jet and its distance from the nozzle exit are about 1·3 and 2·1 nozzle radii at 43,000 feet, but both increase extremely rapidly with altitude above about 150,000 feet and are of the order of 300 and 600 nozzle radii at 400,000 feet. The location and radius of the normal shock behave in an approximately similar manner, and the distance of the shock from the nozzle exit is taken to be about four-thirds the distance of the maximum jet radius and, above 150,000 feet, the radius of the normal shock is taken to be about one-third the maximum radius of the jet. The ratios of the temperature, density and pressure on the jet boundary to the reference values at the nozzle exit vary from unity at 43,000 feet to about 0·2, 0·0001 and 0·00002 respectively at 400,000 feet.

LIST OF SYMBOLS

d		Radius of normal shock
$f_1(M_j)$		Factor used to give effect of axial symmetry in initial slope of Mach number distribution along axis
$f_2(\theta_n, \gamma_j, M_j)$		Factor used to give effect of θ_n in initial slope of Mach number distribution along axis
g		Radius of uniform sonic stream with same mass flow as that through nozzle
h		Altitude in millions of feet
h_1		Value of h at which $p_j/p_b = 1$; depends on the trajectory
l		Distance of normal shock from exit plane of nozzle
p		Static pressure
$p_{\infty 0}$		Atmospheric pressure at sea level
p_∞		Atmospheric pressure at altitude h; also ambient static pressure on external surface of rocket immediately ahead of nozzle exit
$p_{\infty 1}$		Value of p_∞ when $p_j/p_b = 1$
p_b		Static pressure on jet boundary just at nozzle lip; identical with p_∞ for jet expanding into still air
p_j		Static pressure in jet, taken on the nozzle surface immediately ahead of the exit
p_s		Static pressure on axis immediately ahead of normal shock
s	$=$	$(p/p_j)^{(\gamma_j-1)/2\gamma_j}$
s_b	$=$	$(p_b/p_j)^{(\gamma_j-1)/2\gamma_j}$
t_b	$=$	$(p_b/p_j)^{1/2}$
x		Axial co-ordinate, measured from nozzle exit plane
$x_{\max}$		Value of x at position of first maximum of jet
$x_{\max 1}$		Value of $x_{\max}$ when $p_j/p_b = 1$
$\bar{x}$		Value at x at end of radial flow on axis
y		Radial co-ordinate, measured from axis; nozzle exit radius equals unity
$y_{\max}$		Value of y at position of first maximum of jet
$y_{\max 1}$		Value of $y_{\max}$ when $p_j/p_b = 1$
$G(\gamma_j, M_j)$		Initial slope of axial Mach number distribution for single two-dimensional Prandtl-Meyer expansion
M		Mach number

M_∞ Mach number of missile, defined by trajectory; also Mach number on external surface of rocket immediately ahead of nozzle exit

$M_{\infty 1}$ Value of M_∞ when $p_j/p_b = 1$

$(M_{\infty 1})_{\min}$ Minimum value of $M_{\infty 1}$ consistent with existence of 'well-attached' oblique shock at $p_j/p_b = 1$

M_b Mach number on jet boundary just at nozzle lip

M_j Mach number in jet, taken on the nozzle surface immediately ahead of the exit

M_s Mach number on axis immediately ahead of normal shock

$\overline{M}$ Mach number at end of radial flow on axis

$N_j = 2/(\gamma_j - 1)$

$P(M_\infty, \delta_j)$ Function associated with pressure rise through an oblique shock

P_1 Notation for P when $M_\infty = M_{\infty 1}$ and $\delta_j = \theta_n$

$(P_1)_{\min}$ Minimum value of P_1, occurring when $M_{\infty 1} = (M_{\infty 1})_{\min}$

$P_1' = \partial P_1/\partial M_{\infty 1}$

$\dot{P}_1 = \partial P_1/\partial \theta_n$

$S_1 = -d\sigma/ds$ when $s = 1$

$S_0 = -d\sigma/ds$ when $s = 0$

T_b Temperature on the boundary at the nozzle lip

T_j Jet temperature on the nozzle immediately ahead of the nozzle exit

$X = x_{\max 1}/x_{\max}$

$X_{1/3}$ Value of X when $t_b = \frac{1}{3}$

$X_{1/2}$ Value of X when $t_b = \frac{1}{2}$

X_1' Value of $\dfrac{dX}{dt_b}$ when $t_b = 1$

$Y = y_{\max 1}/y_{\max}$

$Y_{1/3}$ Value of Y when $t_b = \frac{1}{3}$

$Y_{1/2}$ Value of Y when $t_b = \frac{1}{2}$

Y_1' Value of $\dfrac{dY}{dt_b}$ when $t_b = 1$

γ_j Ratio of specific heats of jet gas

η = $[1+(M-\bar{M})^{-1}]^{-1}$

θ Angle of inclination (to axis) of streamline at nozzle lip at arbitrary point in Prandtl-Meyer expansion

θ_n Semi-divergence angle of nozzle

θ_b Initial direction angle of jet

θ_{b0} Value of θ_b when $\theta_n = 0$; $\theta_{b0} = \nu_b - \nu_j$

$\theta_{b0\max}$ Value of θ_{b0} when $p_j/p_b = \infty$; $\theta_{b0\max} = (\nu_{\max} - \nu_j)$

λ 'Area-ratio' function

λ_j Value of λ corresponding to M_j

$\bar{\lambda}$ Value of λ corresponding to $\bar{M}$

μ Mach angle

μ_j Value of μ corresponding to M_j

ν Prandtl-Meyer angle

$\nu_{\max}$ Value of ν when $M = \infty$

ν_b Value of ν corresponding to M_b

ν_j Value of ν corresponding to M_j

$\bar{\nu}$ Value of ν corresponding to $\bar{M}$

ξ $1 - [1 + (x - \bar{x})]^{-(\gamma_j - 1)}$

$\xi_{1/2}$ Value of ξ when $\eta = \frac{1}{2}$

ρ_b Density on the boundary at the nozzle lip

ρ_j Jet density on nozzle immediately ahead of nozzle exit

σ $(\nu - \nu_j)/(\nu_{\max} - \nu_j)$

τ Ratio of local speed of sound to stagnation sound speed

τ_j Value of τ corresponding to M_j

τ_b Value of τ corresponding to M_b

ϕ Angle of inclination (to axis) of characteristic in Prandtl-Meyer expansion at nozzle lip

ϕ_b Angle of inclination of curved shock at nozzle lip

REFERENCES

No.	Author(s)	Title, etc.
1	R. F. Clippinger	Supersonic axially symmetric nozzles. B.R.L. Report No. 794. December, 1951.
2	E. S. Love, C. E. Grigsby, L. P. Lee and M. J. Woodling	Experimental and theoretical studies of axisymmetric free jets. N.A.S.A. T.R. R–6. 1959.
3	C. J. Wang and J. B. Peterson ..	Spreading of supersonic jets from axially symmetric nozzles. *Jet Propulsion.* Vol. 28. No. 5. May, 1958.
4	H. Treutler	Private communication. (R. P. E. Westcott.)
5	P. L. Owen and C. K. Thornhill ..	The flow in an axially symmetric supersonic jet from a nearly sonic orifice into a vacuum. A.R.C. R. & M. 2616. September, 1948.
6	M. G. Smith	The behaviour of an axially symmetric sonic jet near to the sonic line. Unpublished M.O.A. Report.
7	E. S. Love, M. J. Woodling and L. P. Lee	Boundaries of supersonic axisymmetric free jets. N.A.C.A. Research Memo. L56G18. TIL 5292. October, 1956.
8	E. S. Love and L. P. Lee	Shape of initial portion of boundary of supersonic axisymmetric free jets at large jet pressure ratios. N.A.C.A. Tech. Note. 4195. January, 1958.
9	T. C. Adamson Jr. and J. A. Nicholls	On the structure of jets from highly under-expanded nozzles into still air. *J. Aero/Space Sci.* Vol. 26, No. 1. January, 1959.
10	E. S. Love	Initial inclination of the mixing boundary separating and exhausting supersonic jet from a supersonic ambient stream. N.A.C.A. Research Memo. L55J14. TIL 4938. January, 1956.
11	E. S. Love	An approximation of the boundary of a supersonic axisymmetric jet exhausting into a supersonic stream. Readers Forum, *J. Ae. Sci.* Vol. 25. No. 2. February, 1958.
12	R. Ladenburg, C. C. Van Vourhis and J. Winckler	Interferometric studies of faster than sound phenomena. Part II.—Analysis of supersonic air jets. *Physical Review.* Vol. 76. No. 5. September, 1949.
13	Ames Research Staff	Equations, Tables and Charts for compressible flow. N.A.C.A. Report 1135. 1953.

REFERENCES—*continued*

No.	*Author(s)*	*Title, etc.*
14	Aeronautical Research Council ..	*A selection of tables for use in calculations of compressible airflow.* Clarendon Press, Oxford, 1952. (Also Graphs, 1954.).
15		Handbook of supersonic aerodynamics. Vol. 2. Navord Report 1488. 1950.
16	K. E. Tempelmeyer and G. H. Sheraden	Compressible flow tables for gases with specific heat ratios from 1·10 to 1·28. AEDC TN–58–9 Astia Document No. AD–152041. March, 1958.
17	Lewis Laboratory Computing Staff ..	Tables of various Mach number functions for specific heat ratios from 1·28 to 1·38. N.A.C.A. Tech. Note 3981. April, 1957.
18	Princeton Univ. Gas Dynamics Lab. Staff	Charts for flow parameters of helium at hypersonic speeds, Mach number 10 to 20. WADC TN–57–377 Astia Document No. AD–142310. November, 1957.
19	R. A. Minzner, W. S. Ripley and T. P. Condron	U.S. extension to the I.C.A.O. standard atmosphere. Tables and data to 300 standard geopotential kilometers. U.S. Govt. Printing Office, Washington D.C. 1958.

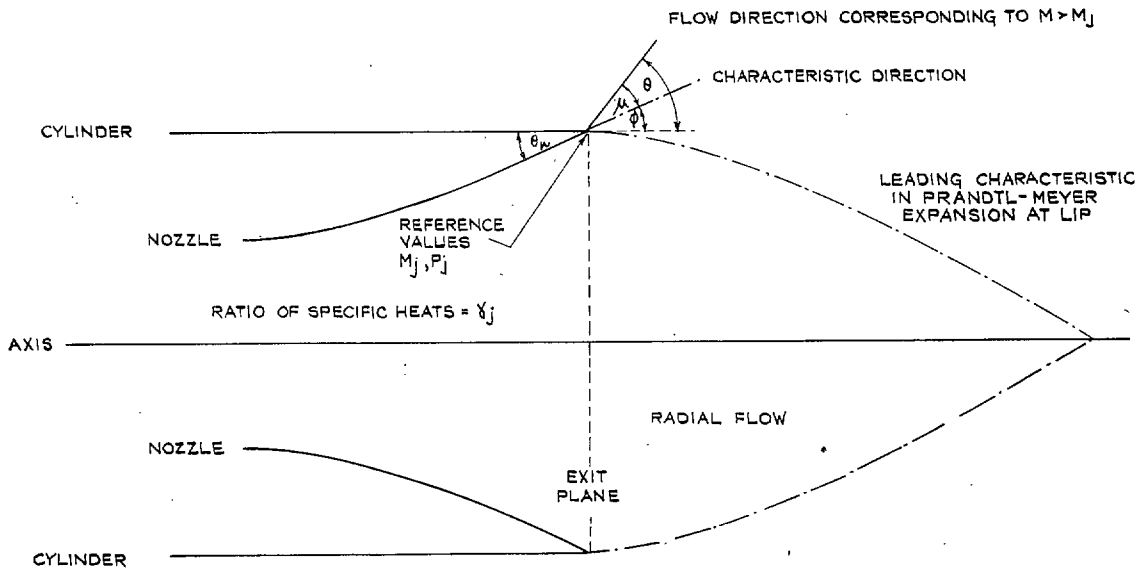

FIG. 1. Details of conditions near the nozzle exit.

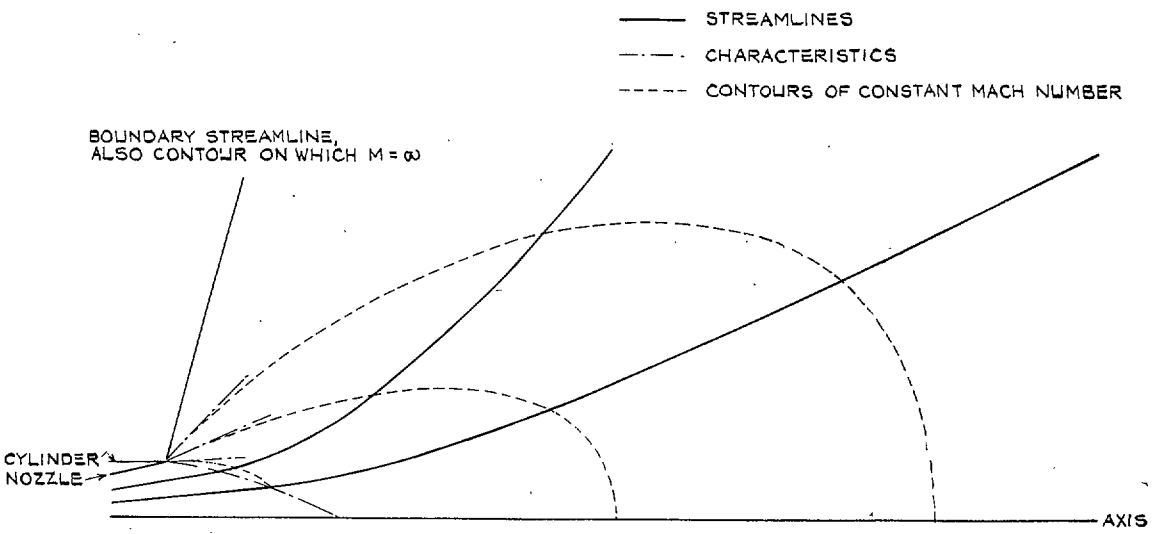

FIG. 2. Sketch of flow field of jet expanding into a vacuum.

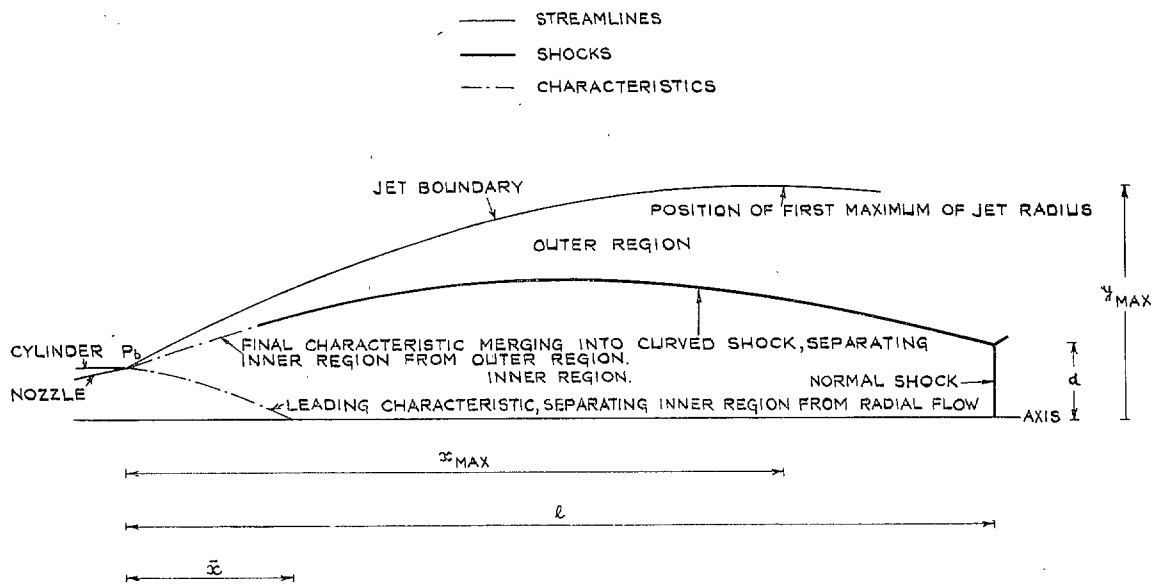

FIG. 3. Sketch of flow field of jet expanding into still air.

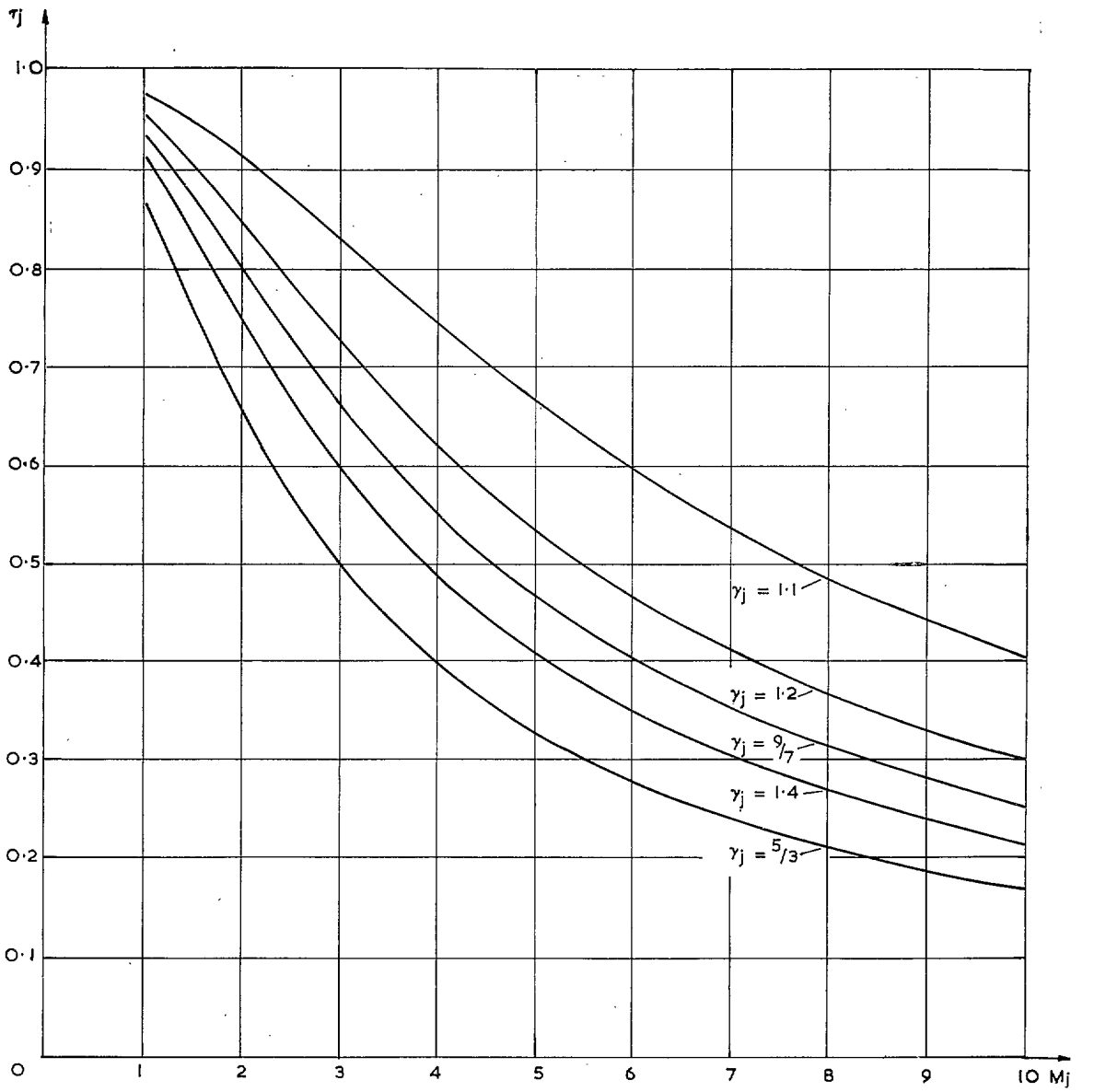

FIG. 4. τ_j as a function of γ_j and M_j.

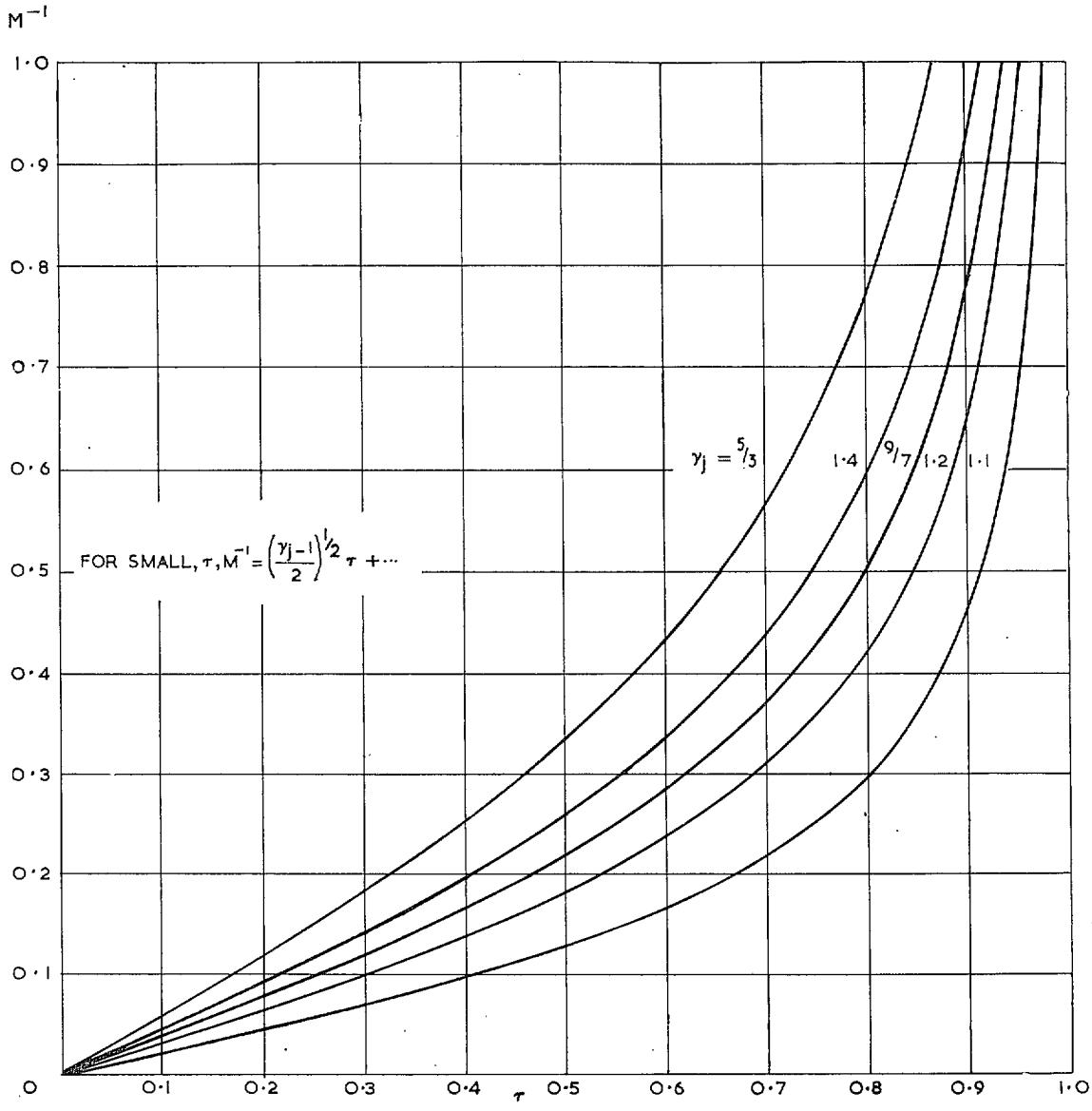

FIG. 5. M^{-1} as a function of γ_j and τ.

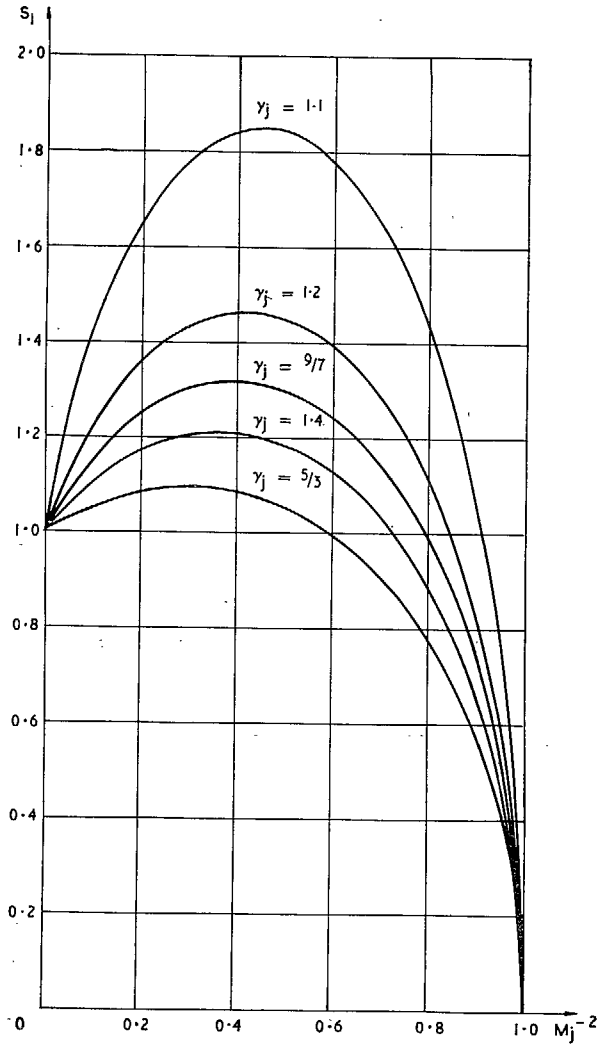

FIG. 6. The function $S_1(\gamma_j, M_j)$.

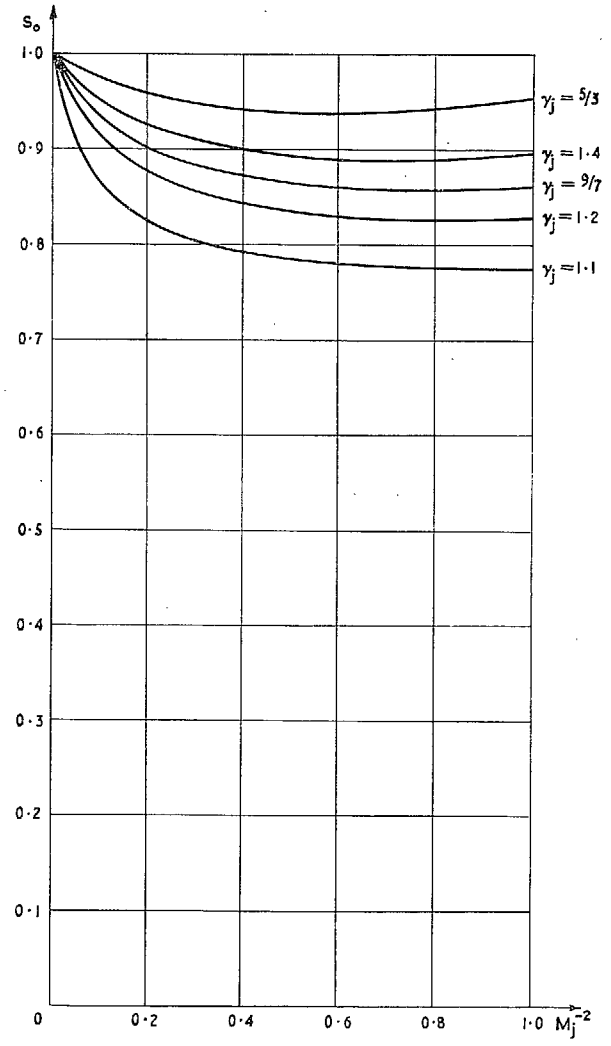

FIG. 7. The function $S_0(\gamma_j, M_j)$.

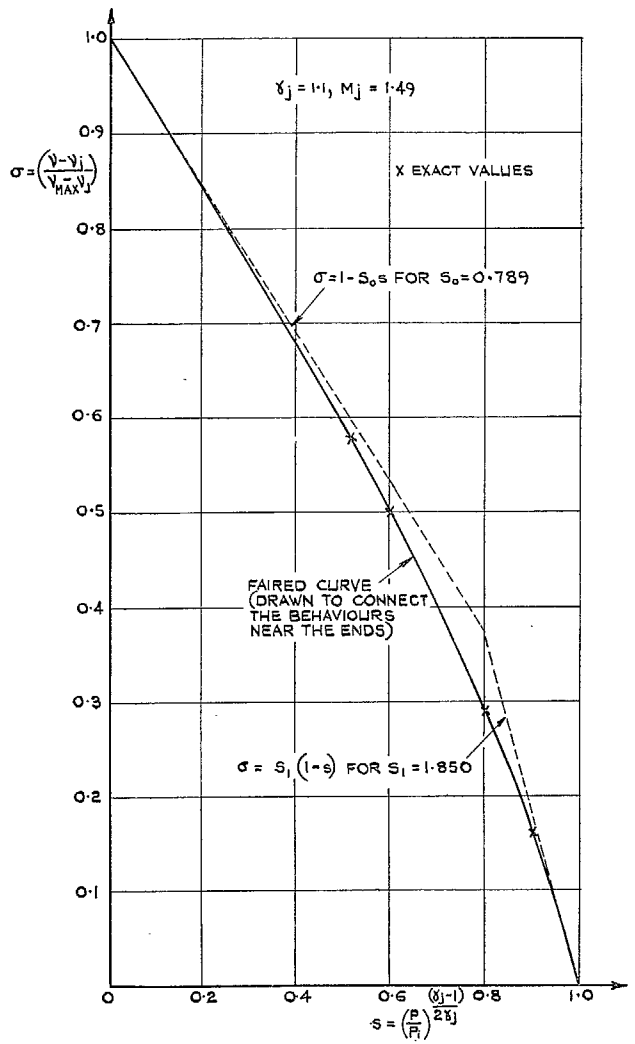

FIG. 8. An example of the approximate method of calculating $(\nu-\nu_j)/(\nu_{\max}-\nu_j) = \sigma$.

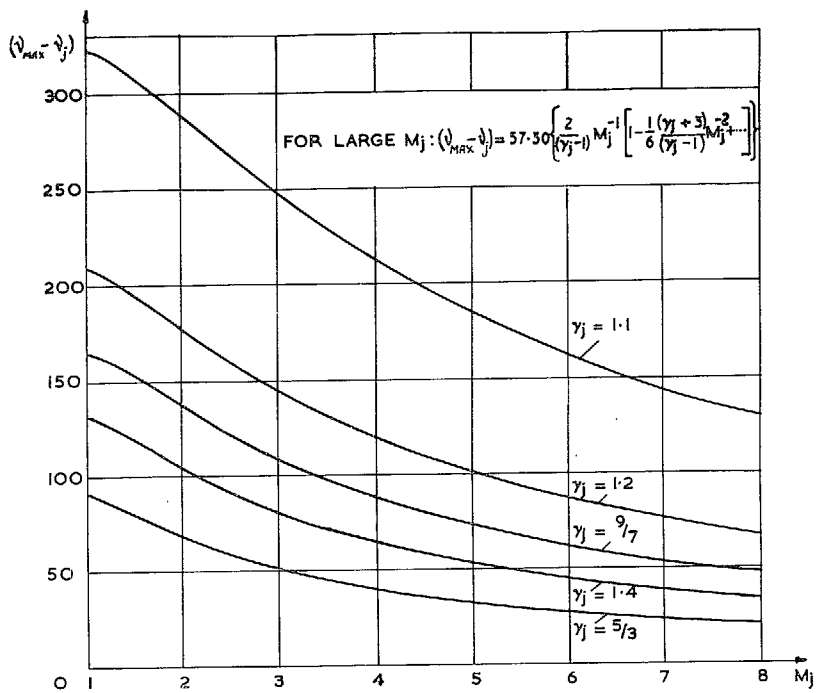

FIG. 9. The function $(\nu_{\max}-\nu_j)$.

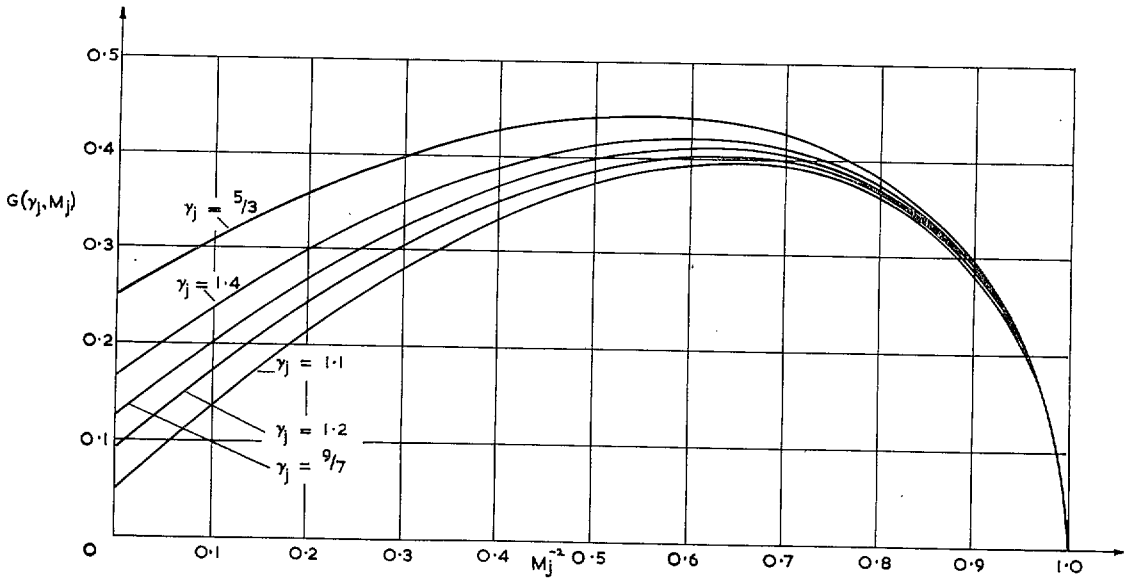

FIG. 10. The function $G(\gamma_j, M_j)$.

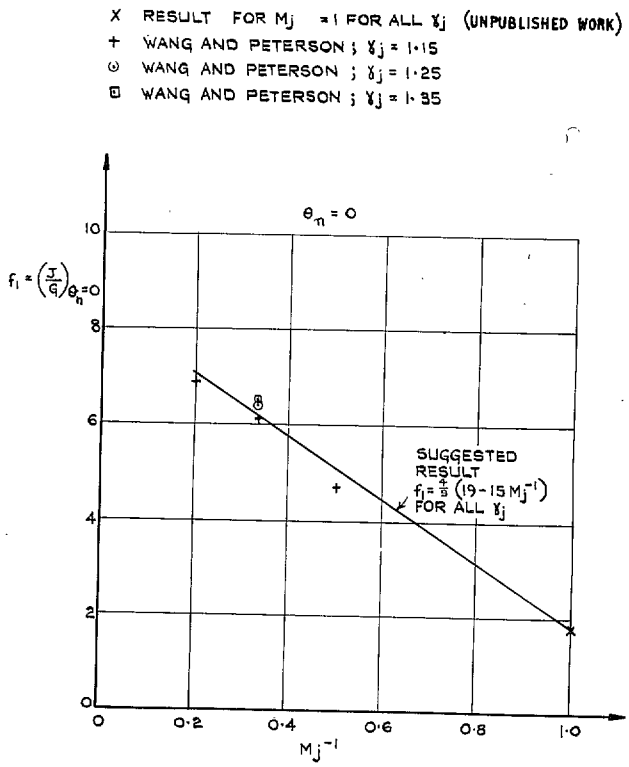

FIG. 11. The factor $f_1(M_j)$.

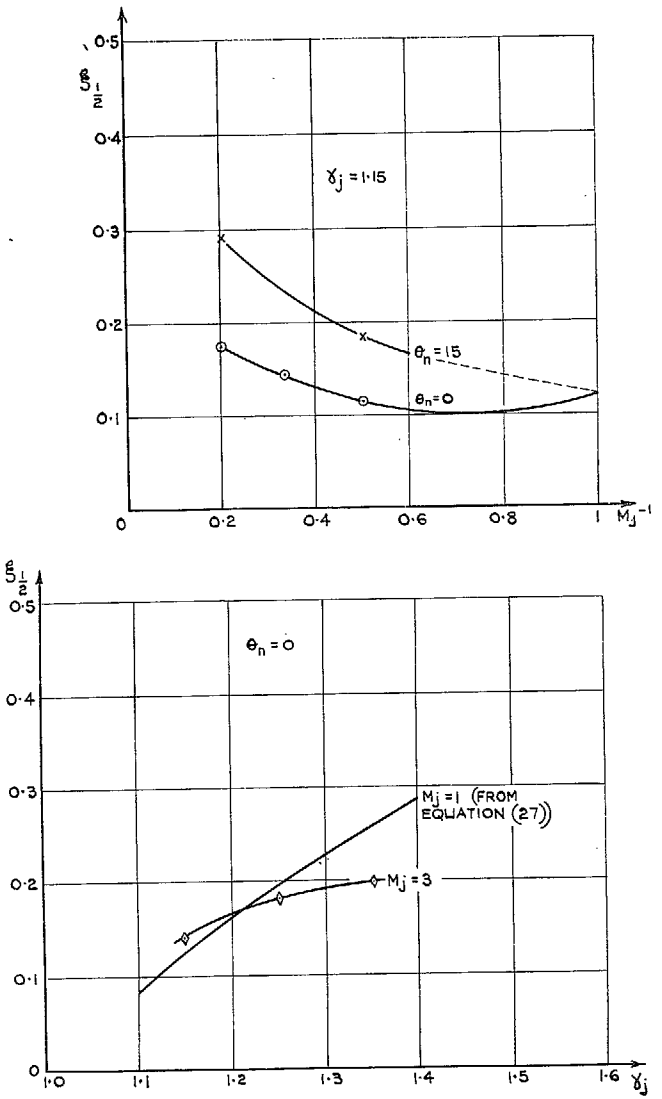

FIG. 12. Some values of $\xi_{1/2}$.

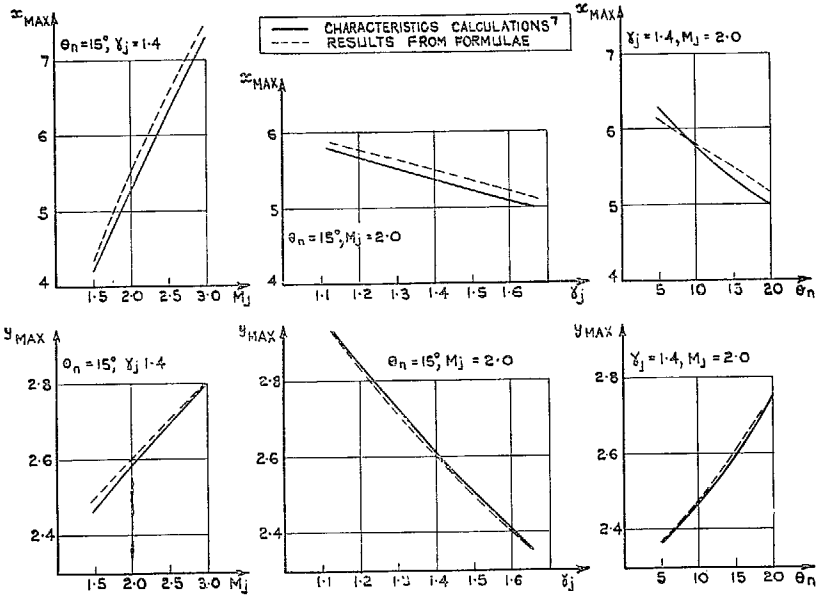

FIG. 13. Comparison of numerical calculations and results from formulae for x_{max}, y_{max}.

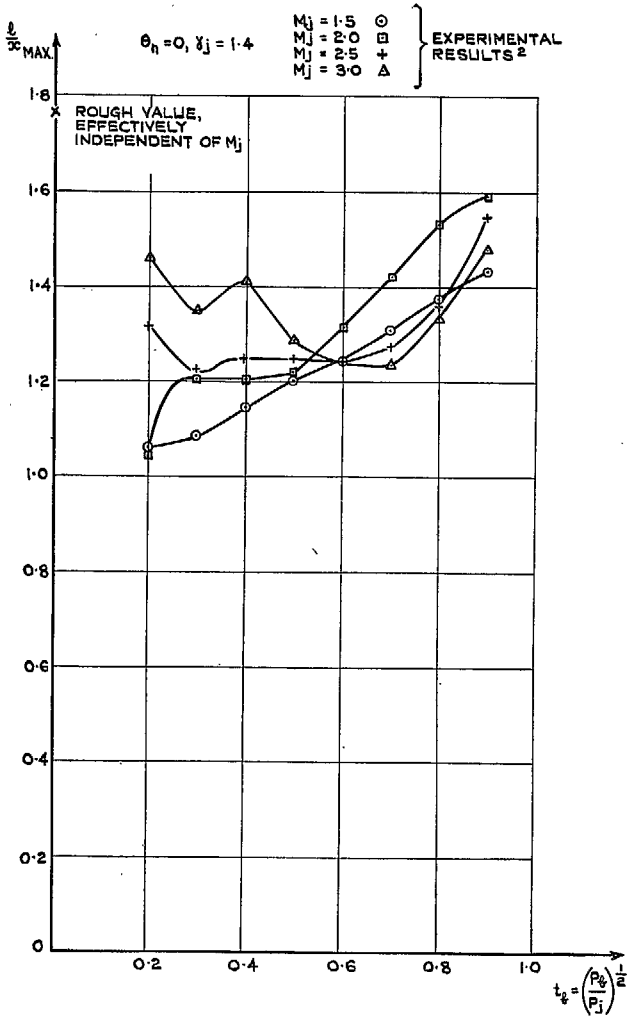

FIG. 14. Some values of $l/x_{\max}$.

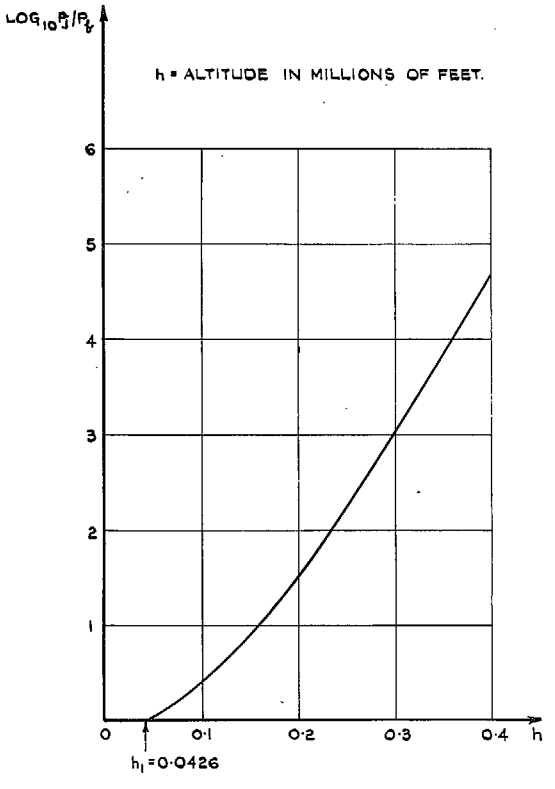

FIG. 15. Example; variation of P_j/P_b with altitude.

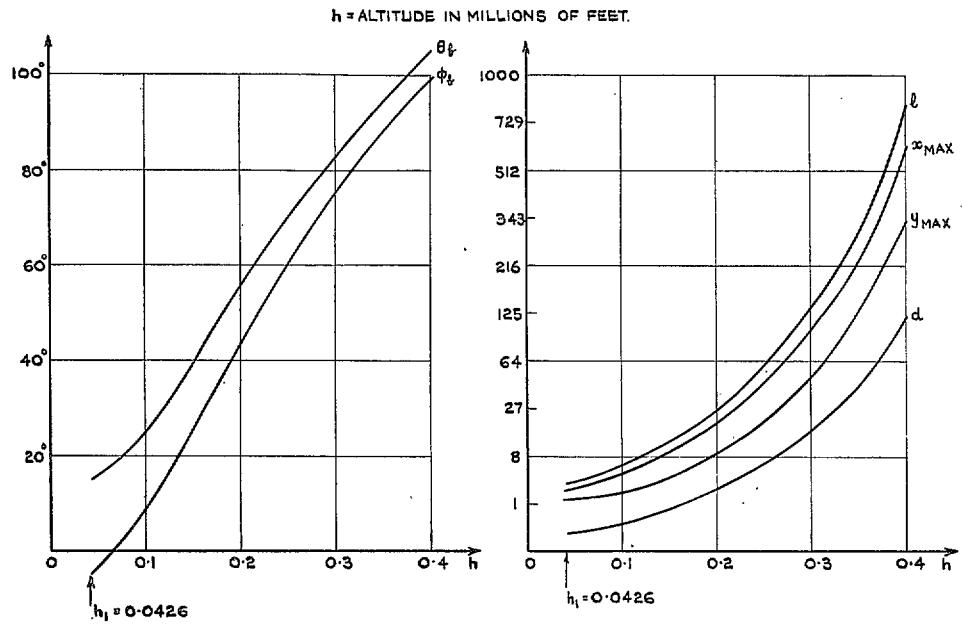

FIG. 16. Example; variations of θ_b, ϕ_b, x_{max}, y_{max}, l, d, with altitude.

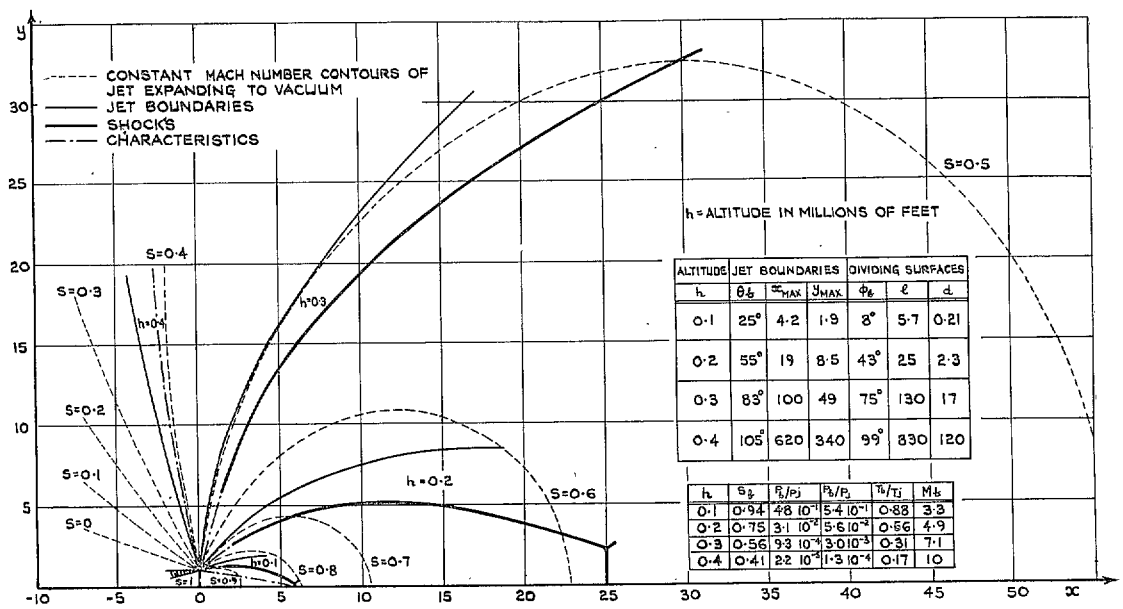

FIG. 17. Example; jet boundaries and shock waves for some particular values of altitudes, superimposed on basic pattern of constant Mach number contours.

(83080) Wt. 67/1876 K5 1/62 Hw.

Publications of the Aeronautical Research Council

ANNUAL TECHNICAL REPORTS OF THE AERONAUTICAL RESEARCH COUNCIL (BOUND VOLUMES)

1941 Aero and Hydrodynamics, Aerofoils, Airscrews, Engines, Flutter, Stability and Control, Structures. 63*s.* (post 2*s.* 3*d.*)

1942 Vol. I. Aero and Hydrodynamics, Aerofoils, Airscrews, Engines. 75*s.* (post 2*s.* 3*d.*)
Vol. II. Noise, Parachutes, Stability and Control, Structures, Vibration, Wind Tunnels. 47*s.* 6*d.* (post 1*s.* 9*d.*)

1943 Vol. I. Aerodynamics, Aerofoils, Airscrews. 80*s.* (post 2*s.*)
Vol. II. Engines, Flutter, Materials, Parachutes, Performance, Stability and Control, Structures. 90*s.* (post 2*s.* 3*d.*)

1944 Vol. I. Aero and Hydrodynamics, Aerofoils, Aircraft, Airscrews, Controls. 84*s.* (post 2*s.* 6*d.*)
Vol. II. Flutter and Vibration, Materials, Miscellaneous, Navigation, Parachutes, Performance, Plates and Panels, Stability, Structures, Test Equipment, Wind Tunnels. 84*s.* (post 2*s.* 6*d.*)

1945 Vol. I. Aero and Hydrodynamics, Aerofoils. 130*s.* (post 3*s.*)
Vol. II. Aircraft, Airscrews, Controls. 130*s.* (post 3*s.*)
Vol. III. Flutter and Vibration, Instruments, Miscellaneous, Parachutes, Plates and Panels, Propulsion. 130*s.* (post 2*s.* 9*d.*)
Vol. IV. Stability, Structures, Wind Tunnels, Wind Tunnel Technique. 130*s.* (post 2*s.* 9*d.*)

1946 Vol. I. Accidents, Aerodynamics, Aerofoils and Hydrofoils. 168*s.* (post 3*s.* 3*d.*)
Vol. II. Airscrews, Cabin Cooling, Chemical Hazards, Controls, Flames, Flutter, Helicopters, Instruments and Instrumentation, Interference, Jets, Miscellaneous, Parachutes. 168*s.* (post 2*s.* 9*d.*)
Vol. III. Performance, Propulsion, Seaplanes, Stability, Structures, Wind Tunnels. 168*s.* (post 3*s.*)

1947 Vol. I. Aerodynamics, Aerofoils, Aircraft. 168*s.* (post 3*s.* 3*d.*)
Vol. II. Airscrews and Rotors, Controls, Flutter, Materials, Miscellaneous, Parachutes, Propulsion, Seaplanes, Stability, Structures, Take-off and Landing. 168*s.* (post 3*s.* 3*d.*)

Special Volumes

Vol. I. Aero and Hydrodynamics, Aerofoils, Controls, Flutter, Kites, Parachutes, Performance, Propulsion, Stability. 126*s.* (post 2*s.* 6*d.*)
Vol. II. Aero and Hydrodynamics, Aerofoils, Airscrews, Controls, Flutter, Materials, Miscellaneous, Parachutes, Propulsion, Stability, Structures. 147*s.* (post 2*s.* 6*d.*)
Vol. III. Aero and Hydrodynamics, Aerofoils, Airscrews, Controls, Flutter, Kites, Miscellaneous, Parachutes, Propulsion, Seaplanes, Stability, Structures, Test Equipment. 189*s.* (post 3*s.* 3*d.*)

Reviews of the Aeronautical Research Council

1939–48 3*s.* (post 5*d.*) 1949–54 5*s.* (post 5*d.*)

Index to all Reports and Memoranda published in the Annual Technical Reports

1909–1947 R. & M. 2600 6*s.* (post 2*d.*)

Indexes to the Reports and Memoranda of the Aeronautical Research Council

Between Nos. 2351–2449	R. & M. No. 2450 2*s.* (post 2*d.*)
Between Nos. 2451–2549	R. & M. No. 2550 2*s.* 6*d.* (post 2*d.*)
Between Nos. 2551–2649	R. & M. No. 2650 2*s.* 6*d.* (post 2*d.*)
Between Nos. 2651–2749	R. & M. No. 2750 2*s.* 6*d.* (post 2*d.*)
Between Nos. 2751–2849	R. & M. No. 2850 2*s.* 6*d.* (post 2*d.*)
Between Nos. 2851–2949	R. & M. No. 2950 3*s.* (post 2*d.*)
Between Nos. 2951–3049	R. & M. No. 3050 3*s.* 6*d.* (post 2*d.*)

HER MAJESTY'S STATIONERY OFFICE

from the addresses overleaf

Printed and published by
HER MAJESTY'S STATIONERY OFFICE

To be purchased from
York House, Kingsway, London W.C.2
423 Oxford Street, London W.1
13A Castle Street, Edinburgh 2
109 St. Mary Street, Cardiff
39 King Street, Manchester 2
50 Fairfax Street, Bristol 1
2 Edmund Street, Birmingham 3
80 Chichester Street, Belfast 1
or through any bookseller

Printed in England

R. & M. No. 3235

S.O. Code No. 23-3235